American Mineralogist, Volume 100, pages 1633–1636, 2015

LETTER

Structural and chemical characterization of $Mg[(Cr,Mg)(Si,Mg)]O_4$, a new post-spinel phase with sixfold-coordinated silicon

LUCA BINDI[1,2,*], EKATERINA A. SIROTKINA[3,4], ANDREY V. BOBROV[3,4] AND TETSUO IRIFUNE[5,6]

[1]Dipartimento di Scienze della Terra, Università di Firenze, Via La Pira 4, I-50121 Firenze, Italy
[2]CNR, Istituto di Geoscienze e Georisorse, sezione di Firenze, Via La Pira 4, I-50121 Firenze, Italy
[3]Department of Petrology, Geological Faculty, Moscow State University, Leninskie Gory, 119234, Moscow, Russia
[4]Vernadsky Institute of Geochemistry and Analytical Chemistry of Russian Academy of Sciences, Moscow, 119991, Russia
[5]Geodynamics Research Center, Ehime University, Matsuyama 790-8577, Japan
[6]Earth-Life Science Institute, Tokyo Institute of Technology, Tokyo 152-8550, Japan

ABSTRACT

The crystal structure and chemical composition of a crystal of $Mg(Mg,Cr,Si)_2O_4$ post-spinel phase synthesized in the model system $MgCr_2O_4$–Mg_2SiO_4 at 16 GPa and 1600 °C have been investigated. The compound was found to crystallize with a distorted orthorhombic calcium-titanate ($CaTi_2O_4$) structure type, space group $Cmc2_1$, with lattice parameters a = 2.8482(1), b = 9.4592(5), c = 9.6353(5) Å, V = 259.59(1) Å^3, and Z = 4. The structure was refined to R_1 = 0.018 using 345 independent reflections. The loss of the inversion center is due to the ordering of cations at the octahedral sites: Cr is mainly hosted at the M1 site, whereas Si at the M2 site. Such an ordered distribution induces a distortion thus provoking a change in coordination of Mg, which becomes sevenfold-coordinated instead of the usual eightfold coordination observed in post-spinel phases. Electron microprobe analysis gave the $Mg[(Cr_{0.792}Mg_{0.208})(Si_{0.603}Mg_{0.397})]O_4$ stoichiometry for the studied phase. The successful synthesis of this phase can provide new constraints on thermobarometry of wadsleyite/ringwoodite-bearing assemblages.

Keywords: Calcium titanate structure, chromium, spinel, post-spinel phases, crystal structure, microprobe analysis, synthesis

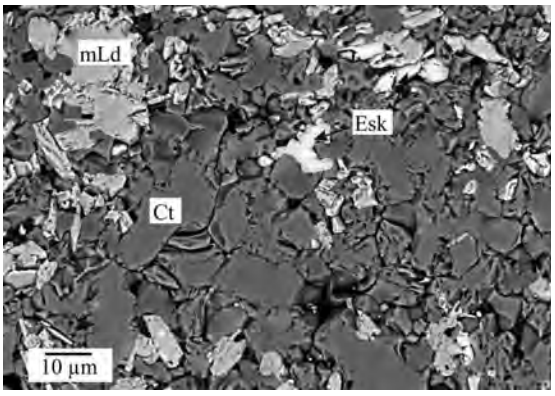

Figure 1. SEM-BSE image of idiomorphic crystals of the new Cr-rich phase studied here (Ct) associated with $Mg_2Cr_2O_5$ (mLd) and eskolaite (Esk) in the run 2629-40 (P = 16 GPa, T = 1600 °C). CamScan electronic microscope MV2300.

Xcalibur 3 diffractometer (X-ray Mo$K\alpha$ radiation, λ = 0.71073 Å) equipped with a Sapphire 2 CCD detector (see Table 1 for details). Intensity integration and standard Lorentz-polarization corrections were performed with the CrysAlis RED (Oxford Diffraction 2006) software package. The program ABSPACK of the CrysAlis RED package (Oxford Diffraction 2006) was used for the absorption correction.

Reflection conditions (hkl: $h + k = 2n$; $0kl$: $k = 2n$; $h0l$: $h,l = 2n$; $hk0$: $h + k = 2n$; $h00$: $h = 2n$; $0k0$: $k = 2n$; $00l$: $l = 2n$) were consistent with the space groups $Cmcm$ and $Cmc2_1$, the first being the space group typically observed in post-spinel phases exhibiting a calcium-titanate structure type (e.g., Yamanaka et al. 2008). Although the statistical tests on the distribution of $|E|$ values strongly indicate the absence of an inversion center ($|E^2 - 1|$ = 0.803), preliminary refinements using the full-matrix least-squares program SHELXL-97 (Sheldrick 2008), were carried out in the space group $Cmcm$ starting from the atomic coordinates reported for the post-spinel phase of $MgCr_2O_4$ (Bindi et al. 2014). The structural model obtained (R = 0.20) indicated a large spread of the electron density around the octahedral site, and the displacement parameters of two of the three oxygen atoms showed non-positive values. At this point, a thorough analysis of the structure (essentially based upon the observation of the displacement parameters for particular atoms) suggested that the mirror symmetry perpendicular to the **c**-axis of the $Cmcm$ space group should be removed. The reflection and atomic position data sets were then adapted to the $Cmc2_1$ space group and the structure refined. The unique octahedral site in the $Cmcm$ space group splits in two octahedra (hereafter M1 and M2) in the non-centrosymmetric $Cmc2_1$ space group. Site-scattering values were refined using scattering curves for neutral species (Ibers and Hamilton 1974) as follows: Mg vs. Cr for the eightfold-coordinated Mg site, Cr vs. □ and Si vs. □ for the M1 and M2 sites, respectively, and O vs. □ for the anion sites. The Mg and O sites were found to be fully occupied, and the occupancy factors were then fixed to 1.00. The refined mean electron numbers at the M1 and M2 sites were found to be 21.65(6) and 12.99(6), respectively, thus indicating an ordering of the smaller light species (i.e., Si) at the M2 site. Such a distribution is also in agreement with the observed sites geometry (see below). Successive cycles were run introducing anisotropic temperature factors for all the atoms leading to R_1 = 0.0182 for 219 observed reflections [$F_o > 4\sigma(F_o)$] and R_1 = 0.0188 for all 345 independent reflections. The Flack parameter of 0.01(2) (Flack 1983) indicated the orientation to be correct. Given the non-centrosymmetric nature of the structure, the possible effect of anomalous dispersion of X-ray was taken into account. For this purpose, a new data collection was carried out using an Oxford Diffraction Excalibur PX Ultra diffractometer equipped with a 165 mm diagonal Onyx CCD detector at 2.5:1 demagnification operating with Cu$K\alpha$ radiation (λ = 1.5406 Å). The refinement results were nearly identical to those obtained using Mo$K\alpha$ radiation either in electron densities at the structural sites and atom coordinates. In the present article, we decided to present data obtained using Mo$K\alpha$ radiation.

Fractional atomic coordinates and atomic displacement parameters are shown in Table 2. Table 3[1] lists the observed and calculated structure factors. Bond distances and geometric parameters are reported in Table 4.

Table 1. Data and experimental details for the selected crystal

Crystal data	
Formula	$Mg(Cr_{0.8}Mg_{0.2})(Si_{0.6}Mg_{0.4})O_4$
Crystal size (mm)	0.035 × 0.042 × 0.048
Form	block
Color	transparent
Crystal system	orthorhombic
Space group	$Cmc2_1$ (no. 36)
a (Å)	2.8482(1)
b (Å)	9.4592(5)
c (Å)	9.6353(5)
V (Å^3)	259.59(2)
Z	4
Data collection	
Instrument	Oxford Diffraction Xcalibur 3
Radiation type	Mo$K\alpha$ (λ = 0.71073 Å)
Temperature (K)	293(2)
Detector to sample distance (cm)	6
Number of frames	2024
Measuring time (s)	130
Maximum covered 2θ (°)	69.60
Absorption correction	multi-scan (ABSPACK; Oxford Diffraction 2006)
Collected reflections	4529
Unique reflections	345
Reflections with $F_o > 4\sigma(F_o)$	219
R_{int}	0.0214
R_σ	0.0408
Range of h, k, l	$-4 \le h \le 4$, $-15 \le k \le 15$, $-15 \le l \le 15$
Refinement	
Refinement	Full-matrix least squares on F^2
Final R_1 [$F_o > 4\sigma(F_o)$]	0.0182
Final R_1 (all data)	0.0188
Flack parameter	0.01(2)
Number of least-squares parameters	45
Goodness of fit	1.045
$\Delta\rho_{max}$ (e/Å^3)	0.60
$\Delta\rho_{min}$ (e/Å^3)	–0.85

Chemical composition

A preliminary chemical analysis using energy-dispersive spectrometry, performed on the same crystal fragment used for the structural study as well as on other fragments from the same run product, did not indicate the presence of elements (Z > 9) other than Cr, Mg, and Si. The chemical composition was then determined using wavelength-dispersive analysis (WDS) by means of a Jeol JXA-8600 electron microprobe. We used 40 s as counting time. The matrix correction was performed with the Bence and Albee (1968) program as modified by Albee and Ray (1970). The standards employed were forsterite (Mg, Si) and synthetic Cr_2O_3 (Cr). The crystal used for the X-ray study was found to be homogeneous within the analytical uncertainty. The average chemical composition (six analyses on different spots) is (wt%), SiO_2 22.4(2); Cr_2O_3 37.3(3); MgO 40.1(3); total 99.8(3); corresponding, on the basis of four oxygen atoms, to $Mg_{1.606(5)}Cr_{0.792(6)}Si_{0.603(5)}O_4$.

Results and discussion

$Mg(Cr,Mg)(Si,Mg)O_4$ crystallizes with a distorted orthorhombic calcium-titanate ($CaTi_2O_4$) structure type (Fig. 2), space group $Cmc2_1$, with lattice parameters a = 2.8482(1), b = 9.4592(5), c = 9.6353(5) Å, V = 259.59(2) Å^3, and Z = 4. The departure from the classic $Cmcm$ space group is due to the ordering of the octahedral cations, which is required to either account for the electron density at those sites and justify the variation of the octahedral bond distances (Table 4). In detail, Cr (with minor Mg) is mainly hosted at the M1 site and Si (with minor Mg) is hosted at the M2 site, whereas the eightfold-coordinated site is fully occupied by Mg. The linkage among the octahedra is provided by edge and corner sharing.

The bond distances of the M1 and M2 octahedra show a large anisotropy being in the range 1.950–2.165 and 1.878–1.985 Å, respectively. M1, mainly occupied by Cr, exhibits a mean

[1] Deposit item AM-15-75322, Table 3 and CIF. Deposit items are free to all readers and found on the MA web site, via the specific issue's Table of Contents (go to http://www.minsocam.org/MSA/AmMin/TOC/).

TABLE 2. Atoms, atom coordinates, and atomic displacement parameters (Å^2) for the selected crystal

Atom	s.o.f.	*x*	*y*	*z*	U_{11}	U_{22}	U_{33}	U_{23}	U_{13}	U_{12}	U_{iso}*/U_{eq}
Mg	$Mg_{1.000}$	0	0.3785(2)	0.2487(2)	0.0184(8)	0.0247(9)	0.0253(6)	–0.001(1)	0	0	0.0228(4)
M1	$Cr_{0.804(4)}Mg_{0.196}$	0	0.1289(1)	0.06852(4)	0.0192(5)	0.0234(4)	0.0227(5)	–0.001(1)	0	0	0.0218(3)
M2	$Si_{0.495(8)}Mg_{0.505}$	0	0.8547(2)	0.9274(1)	0.023(1)	0.026(1)	0.025(1)	–0.0028(7)	0	0	0.0250(6)
O1	$O_{1.000}$	0	0.4971(5)	–0.0405(2)	0.027(2)	0.034(2)	0.032(2)	–0.001(2)	0	0	0.0310(9)
O2	$O_{1.000}$	0	0.0394(3)	0.2508(4)	0.027(2)	0.031(2)	0.030(1)	–0.001(2)	0	0	0.0292(8)
O3	$O_{1.000}$	0	0.2313(5)	0.8893(4)	0.025(3)	0.037(3)	0.032(2)	0.001(2)	0	0	0.031(1)
O4	$O_{1.000}$	0	0.7659(5)	0.1087(3)	0.023(3)	0.031(2)	0.030(2)	–0.001(2)	0	0	0.028(1)

bond distance of 2.031 Å (Table 4), which is slightly greater than that found in eskolaite, Cr_2O_3 (1.988 Å; Ovsyannikov and Dubrovinsky 2011), that observed for ^{VI}Cr in synthetic $MgCr_2O_4$ with spinel structure (1.998 Å; O'Neill and Dollase 1994) and that observed for synthetic $MgCr_2O_4$ with post-spinel structure (1.986 Å; Bindi et al. 2014), due to the presence of Mg at the site. The observed value is in excellent agreement with that obtained by the sum of the ionic radii (2.037 Å; Shannon 1976). The Mg–for–Cr substitution at the M1 site induces a distortion with an increase of the octahedral angle variance σ^2 (Robinson et al. 1971) from 15.78 in pure $MgCr_2O_4$ (Bindi et al. 2014) to 60.18 in the studied crystal.

TABLE 4. Selected bond distances (Å) and geometric parameters for the studied crystal

Mg polyhedron	
Mg-O2 (×2)	2.084(3)
Mg-O3 (×2)	2.223(4)
Mg-O4 (×2)	2.232(3)
Mg-O1	2.347(4)
Mg-O1	3.004(3)
^{VIII}<Mg-O>	2.304
^{VIII}V (Å^3)	20.73
^{VII}<Mg-O>	2.204
^{VII}V (Å^3)	14.36
M1 octahedron (Cr,Mg)	
M1-O2	1.950(4)
M1-O4 (×2)	1.964(4)
M1-O3	1.980(4)
M1-O1 (×2)	2.165(3)
<M1-O>	2.031
V (Å^3)	10.89
σ^2	60.18
λ	1.0197
M2 octahedron (Si,Mg)	
M2-O3 (×2)	1.878(4)
M2-O4	1.938(4)
M2-O2	1.975(4)
M2-O1 (×2)	1.985(3)
<M2-O>	1.940
V (Å^3)	9.41
σ^2	71.25
λ	1.0227

Note: Quadratic elongation (λ) and angle variance (σ^2) calculated according to Robinson et al. (1971).

The M2 site population, derived from electron microprobe, can be written as $Si_{0.603}Mg_{0.397}$. Such a distribution slightly differs from that derived from the structure refinement (i.e., $Si_{0.495}Mg_{0.505}$), but it should be kept in mind that the calculated mean electron numbers are very similar (13.7 vs. 13.0) and that elements having similar scattering factors are present. The M2 mean bond distance of 1.940 Å is obviously greater than that observed in pure $MgSiO_3$ (1.793 Å; Dobson and Jacobsen 2004), that observed for ^{VI}Si in synthetic $Na_2MgSi_5O_{12}$ garnet (1.793 Å; Bindi et al. 2011) and that in stishovite (1.757 Å; Hill et al. 1983), due to the presence of significant amounts of Mg. Taking into account the ionic radii (Shannon 1976), values of 1.927 and 1.962 Å can be calculated from the two distributions (obtained by electron microprobe and from the structure refinement, respectively), which are in excellent agreement with the observed value (1.940 Å).

The Mg-polyhedron is very distorted and coordinates seven oxygen atoms at distances shorter than 2.4 Å, with an additional bond at 3.0 Å (Fig. 3a). This feature, together with the cation ordering occurring at the octahedral sites, represents the main difference with respect to the undistorted *Cmcm* calcium-titanate structure where the medium-sized A cations (A = Fe^{2+}, Mg, Co, Zn)

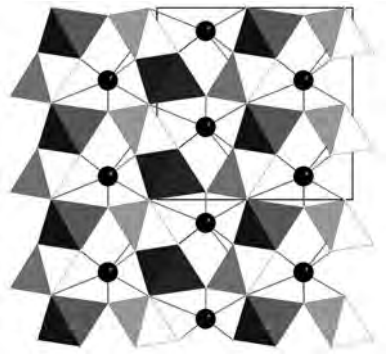

FIGURE 2. The crystal structure of $Mg(Cr,Mg)(Si,Mg)O_4$ projected down [100]. M1 (Cr,Mg) and M2 (Si,Mg) cations are depicted as dark gray and white polyhedra, respectively, whereas the eightfold-coordinated Mg cations as black spheres. The unit cell is outlined. The vertical axis is the *b*-axis.

FIGURE 3. Coordination environment of the Mg polyhedron in the crystal structure of $Mg(Cr,Mg)(Si,Mg)O_4$ (**a**) and in $MgCr_2O_4$ (**b**, Bindi et al. 2014). Colors as in Figure 2. The long Mg-O1 bond distance in the structure of $Mg(Cr,Mg)(Si,Mg)O_4$ is indicated with a dashed line.

coordinate eight oxygen atoms at distances shorter than 2.7–2.8 Å (Fig. 3b). If we consider also the long bond at 3.0 Å with O1, the average Mg-O distance is 2.304 Å. Such a value is slightly greater than that observed for the pure Mg site in the orthorhombic calcium ferrite-type $MgAl_2O_4$ (2.259 Å; Kojitani et al. 2007), and that obtained by the sum of the ionic radii (2.270 Å; Shannon 1976), whereas it is closer to that observed in the tetragonal structure of synthetic $MgSiO_3$ garnet (2.284 Å; Angel et al. 1989).

The bond valence sums calculated using the parameters given by Brese and O'Keeffe (1991) are 1.80(2), 2.70(2), and 2.91(3) for the Mg, M1, and M2 sites, respectively, thus corroborating either the trivalent state for Cr and the proposed cation distribution at the structural sites.

IMPLICATIONS

Since magnesiochromite-rich spinel is commonly reported as inclusions in diamonds, the successful synthesis of the new post spinel phase $Mg[(Cr,Mg)(Si,Mg)]O_4$ with a symmetry different from either the cubic $Fd\bar{3}m$ typical of spinel or the *Cmcm* typical

of calcium-titanate post-spinel is of key importance, because it could represent an important ultrahigh-pressure marker for diamond formation using for example the elastic geobarometry as showed by Angel et al. (2014). Our results are directly applicable to the phase associations of podiform chromitites in the Luobusa ophiolite (Southern Tibet) containing diamond and other former ultrahigh-pressure minerals, such as precursor stishovite for blade-shaped coesite (Yang et al. 2007) and ringwoodite as a precursor of altered Mg–Fe silicate with an octahedral shape (Robinson et al. 2004). Yamamoto et al. (2009) suggested a UHP precursor with a calcium ferrite structure originally formed at a pressure of >12.5 GPa and then decomposed to low-pressure chromite containing silicate exsolutions. Ishii et al. (2015) suggested a lower pressure origin of these chromitites because of the absence of the assemblage $Mg_2Cr_2O_5$ + Cr_2O_3 ($Fe_2Cr_2O_5$ + Cr_2O_3) in them. The new Cr-rich phase synthesized at 16 GPa and 1600 °C, containing significant amounts of the Mg_2SiO_4 component never reported before in a post-spinel phase may be an intermediate product in deep recycling of silicate-bearing UHP chromitites (Arai 2013). Exsolution silicate lamellae in chromite might be formed by inverse transformation from the new post spinel phase Mg[(Cr,Mg)(Si,Mg)]O_4 to chromite during mantle upwelling. Moreover, its structural characterization is crucial for thermodynamic calculations of phase equilibria in the mantle systems, which can provide new constraints on thermobarometry of wadsleyite/ringwoodite-bearing assemblages. Further experimental studies are required to evaluate the compositional range and *P-T* stability of this phase.

Acknowledgments

The paper benefited by the official reviews made by Matteo Alvaro and two anonymous reviewers. Thanks are also due to the Editor Ian Swainson for his efficient handling of the manuscript. The research was supported by "progetto di Ateneo 2013, University of Firenze" to L.B., by C.N.R., Istituto di Geoscienze e Georisorse sezione di Firenze, Italy, the Russian Foundation for Basic Research (project no. 15-55-50033 YaF) to E.S. and A.B. E.S. thanks Geodynamics Research Center, Ehime University, Matsuyama, Japan, for support of her visit in 2014.

References cited

Albee, A.L., and Ray, L. (1970) Correction factors for electron probe analysis of silicate, oxides, carbonates, phosphates, and sulfates. Analytical Chemistry, 48, 1408–1414.

Angel, R.J., Finger, L.W., Hazen, R.M., Kanzaki, M., Weidner, D.J., Liebermann, R.C., and Veblen, D.R. (1989) Structure and twinning of single-crystal $MgSiO_3$ garnet synthesized at 17 GPa and 1800 °C. American Mineralogist, 74, 509–512.

Angel, R.J., Mazzucchelli, M.L., Alvaro, M., Nimis, P., and Nestola, F. (2014) Geobarometry from host-inclusion systems: the role of elastic relaxation. American Mineralogist, 99, 2146–2149.

Arai, S. (2013) Conversion of low-pressure chromitites to ultrahigh-pressure chromitites by deep recycling: a good inference. Earth and Planetary Science Letters, 379, 81–87.

Bence, A.E., and Albee, A.L. (1968) Empirical correction factors for the electron microanalysis of silicate and oxides. Journal of Geology, 76, 382–403.

Biagioni, C., and Pasero, M. (2014) The systematics of the spinel-type minerals: An overview. American Mineralogist, 99, 1254–1264.

Bindi, L., Dymshits, A.M., Bobrov, A.V., Litasov, K.D., Shatskiy, A.F., Ohtani, E., and Litvin, Y.A. (2011) Crystal chemistry of sodium in the Earth's interior: The structure of $Na_2MgSi_5O_{12}$ synthesized at 17.5 GPa and 1700 °C. American Mineralogist, 96, 447–450.

Bindi, L., Sirotkina, E., Bobrov, A.V., and Irifune, T. (2014) X-ray single-crystal structural characterization of $MgCr_2O_4$, a post-spinel phase synthesized at 23 GPa and 1600 °C. Journal of Physics and Chemistry of Solids, 75, 638–641.

Brese, N.E., and O'Keeffe, M. (1991) Bond-valence parameters for solids. Acta Crystallographica, B47, 192–197.

Dobrzhinetskaya, L., Wirth, R., Yang, J.-S., Hutcheon, I., Weber, P., and Green, H.W. (2009) High pressure highly reduced nitride sand oxides from chromite of a Tibetan ophiolite. Proceedings of the National Academy of Sciences, 106, 19233–19238.

Dobson, D.P., and Jacobsen, S.D. (2004) The flux growth of magnesium silicate perovskite single crystals. American Mineralogist, 89, 807–811.

Flack, H.D. (1983) On enantiomorph-polarity estimation. Acta Crystallographica, A39, 876–881.

Hill, R.J., Newton, M.D., and Gibbs, G.V. (1983) A crystal chemical study of stishovite. Journal of Solid State Chemistry, 47, 185–200.

Ibers, J.A., and Hamilton, W.C., Eds. (1974) International Tables for X-ray Crystallography, vol. IV, 366 p. Kynock, Dordrecht, The Netherlands.

Irifune, T., Fujino, F., and Ohtani, E. (1991) A new high-pressure form of $MgAl_2O_4$. Nature, 349, 409–411.

Irifune, T., Kurio, A., Sakamoto, S., Inoue, T., Sumiya. H., and Funakoshi, K. (2004) Formation of pure polycrystalline diamond by direct conversion of graphite at high pressure and high temperature. Physics of the Earth and Planetary Interiors, 143-144, 593–600.

Ishii, T., Kojitani, H., Fujino, K., Yusa, H., Mori, D., Inaguma, Y., Matsushita, Y., Yamaura, K., and Akaogi, M. (2015) High-pressure high-temperature transitions in $MgCr_2O_4$ and crystal structures of new $Mg_2Cr_2O_5$ and post-spinel $MgCr_2O_4$ phases with implications for ultra-high pressure chromitites in ophiolites. American Mineralogist, 100, 59–65.

Katsura, T., and Ito, E. (1989) The system Mg_2SiO_4-Fe_2SiO_4 at high pressure and temperatures: Precise determination of stabilities of olivine, modified spinel, and spinel. Journal of Geophysical Research, 94, 15663–15670.

Kojitani, H., Katsura, T., and Akaogi, M. (2007) Aluminum substitution mechanisms in perovskite-type $MgSiO_3$: An investigation by Rietveld analysis. Physics and Chemistry of Minerals, 34, 257–267.

Lenaz, D., Logvinova, A.M., Princivalle, F., and Sobolev, N. (2009) Structural parameters of chromite included in diamond and kimberlites from Siberia: a new tool for discriminating source. American Mineralogist, 94, 1067–1070.

O'Neill, H.St.C., and Dollase, W.A. (1994) Crystal structures and cation distributions in simple spinels from powder XRD structural refinements: $MgCr_2O_4$, $ZnCr_2O_4$, Fe_3O_4, and the temperature dependence of the cation distribution in $ZnAl_2O_4$. Physics and Chemistry of Minerals, 20, 541–555.

Ovsyannikov, S., and Dubrovinsky, L. (2011) High-pressure high-temperature synthesis of Cr_2O_3 and Ga_2O_3. High Pressure Research, 31, 23–29.

Oxford Diffraction (2006) CrysAlis RED (Version 1.171.31.2) and ABSPACK in CrysAlis RED. Oxford Diffraction, Abingdon, Oxfordshire, U.K.

Robinson, K., Gibbs, G.V., and Ribbe, P.H. (1971) Quadratic elongation: a quantitative measure of distortion in coordination polyhedra. Science, 172, 567–570.

Robinson, P.T., Bai, W.-J., Malpas, J., Yang, J.-S., Zhou, M.F., Fang, Q.-S., Hu, X.-F., Cameron, S., and Staudigel, H. (2004) Ultrahigh-pressure minerals in the Luobusa ophiolite, Tibet, and their tectonic implications. In J. Malpas, C.J.N. Fletcher, J.R. Ali, and J.C. Aitchison, Eds., Aspects of the Tectonic Evolution of China. Journal of Geological Society Special Publication, 226, 247–271.

Shannon, R.D. (1976) Revised effective ionic radii and systematic studies of interatomic distances in halides and chalcogenides. Acta Crystallographica, A32, 751–767.

Sheldrick, G.M. (2008) A short history of SHELX. Acta Crystallographica, A64, 112–122.

Sirotkina, E.A., Bobrov, A.V., Bindi, L., and Irifune, T. (2015) Phase relations and formation of chromium-rich phases in the system $Mg_4Si_4O_{12}$–$Mg_3Cr_2Si_3O_{12}$ at 10–24 GPa and 1,600 °C. Contributions to Mineralogy and Petrology, 169, http://dx.doi.org/10.1007/s00410-014-1097-0.

Yamada, A., Inoue, T., and Irifune, T. (2004) Melting of enstatite from 13 to 18 GPa under hydrous conditions. Physics of the Earth and Planetary Interiors, 147, 45–56.

Yamamoto, S., Kojima, T., Hirose, K., and Maruyama, S. (2009) Coesite and clinopyroxene exsolution lamella in chromites: *In-situ* ultrahigh-pressure evidence from podiform chromitites in the Luobusa ophiolite, southern Tibet. Lithos, 109, 314–322.

Yamanaka, T., Uchida, A., and Nakamoto, Y. (2008) Structural transition of post-spinel phases $CaMn_2O_4$, $CaFe_2O_4$, and $CaTi_2O_4$ under high pressures up to 80 GPa. American Mineralogist, 93, 1874–1881.

Yang, J.S., Dobrzhinetskaya, L., Bai, W.J., Fang, Q.S., Robinson, P.T., Zhang, J., and Green, H.W. (2007) Diamond- and coesite-bearing chromitites from the Luobusa ophiolite, Tibet. Geology, 35, 875–878.

Yong, W., Botis, S., Shieh, S.R., Shi, W., and Withers, A.C. (2012) Pressure-induced phase transition study of magnesiochromite ($MgCr_2O_4$) by Raman spectroscopy and X-ray diffraction. Physics of the Earth and Planetary Interiors, 196-197, 75–82.

Wang, Z., O'Neill, H.St.C., Lazor, P., and Saxena, S.K. (2002) High pressure Raman spectroscopy study of spinel $MgCr_2O_4$. Journal of Physics and Chemistry of Solids, 63, 2057–2061.

Manuscript received February 8, 2015
Manuscript accepted March 19, 2015
Manuscript handled by Ian Swainson